Global MHD simulations of Saturn's magnetosphere at the time of Cassini approach

K. C. Hansen,[1] A. J. Ridley,[1] G. B. Hospodarsky,[2] N. Achilleos,[3] M. K. Dougherty,[3] T. I. Gombosi,[1] and G. Tóth[1]

Received 28 February 2005; revised 13 May 2005; accepted 9 June 2005; published 19 July 2005.

[1] We present the results of a 3D global magnetohydrodynamic simulation of the magnetosphere of Saturn for the period of Cassini's initial approach and entry into the magnetosphere. We compare calculated bow shock and magnetopause locations with the Cassini measurements. In order to match the measured locations we use a substantial mass source due to the icy satellites ($\sim 1 \times 10^{28}$ s^{-1} of water product ions). We find that the location of bow shock and magnetopause crossings are consistent with previous spacecraft measurements, although Cassini encountered the surfaces further from Saturn than the previously determined average location. In addition, we find that the shape of the model bow shock and magnetopause have smaller flaring angles than previous models and are asymmetric dawn-to-dusk. Finally, we find that tilt of Saturn's dipole and rotation axes results in asymmetries in the bow shock and magnetopause and in the magnetotail being hinged near Titan's orbit ($\sim 20\ R_S$). **Citation:** Hansen, K. C., A. J. Ridley, G. B. Hospodarsky, N. Achilleos, M. K. Dougherty, T. I. Gombosi, and G. Tóth (2005), Global MHD simulations of Saturn's magnetosphere at the time of Cassini approach, *Geophys. Res. Lett.*, *32*, L20S06, doi:10.1029/2005GL022835.

1. Introduction

[2] Cassini's arrival at Saturn was marked by the first crossings of the Kronian bow shock and magnetopause since Voyager 2 exited the magnetosphere on 31 August 1981. These new measurements, and those that will be made during the next four years, will add to those made by Pioneer 11, Voyager 1 and Voyager 2 and will extend our knowledge and understanding of the shape and size of the Kronian magnetosphere. Previously, Pioneer and Voyager crossings, together with gas dynamic modeling, were used to develop bow shock (BS) and magnetopause (MP) models [*Slavin et al.*, 1985] that are still the standard today. In the same paper, axisymmetric gas dynamic modeling of the plasma flow around a predefined MP surface provided the first calculation of the shape of the BS and the flow in the magnetosheath. This work was later extended to 3D by *Stahara et al.* [1989]. In addition to these first models, a parameterized model of the MP based on pressure balance and models of the internal field and the ring current has been developed [*Maurice et al.*, 1996]. Though valuable, none of these models addresses the global magnetospheric structure self consistently. *Hansen et al.* [2000] was the first to develop such a model using MHD to study the global solar wind–magnetosphere interaction at Saturn. In this paper we extend the work of *Hansen et al.* [2000] by modeling the magnetosphere of Saturn under conditions appropriate for the period just before the Cassini orbit insertion (26–29 July 2004).

2. Cassini Observations

[3] In order to model the magnetosphere of Saturn we have used Cassini data both to set the upstream boundary of the simulation and for comparison with the model. In principle, using different satellites for setting the boundary conditions and for model–data comparison would be preferred, however Cassini is the only spacecraft near Saturn. Because Cassini data is used to set the boundary condition, one would expect the model and data to show excellent agreement when Cassini is in the solar wind. For these periods, good agreement indicates that the propagation from the upstream boundary to Cassini is being handled correctly. When Cassini crosses the BS into the magnetosheath, the timing of the crossings and the measured magnetosheath conditions serve to validate the model.

[4] During the period modeled, Cassini's orientation was based on navigational, rather than scientific, needs. As a result, the Cassini Plasma Spectrometer instrument was not able to measure the solar wind density, velocity or temperature. Once per hour, the Radio and Plasma Wave Science (RPWS) instrument has wide band data from which we compute the plasma density in the solar wind using the Langmuir wave frequencies [*Gurnett et al.*, 2005]. We linearly interpolate between data points to set the upstream boundary condition. Because we do not know the solar wind speed, we treat this quantity as a free parameter. We use the temperature measured by Cassini during the January 2004 measurements of the solar wind (2×10^4 K) when Cassini was $\sim 1300 R_S$ upstream of Saturn [*Crary et al.*, 2005]. Data from the magnetometer (MAG) is available during the period we are studying at one minute resolution [*Dougherty et al.*, 2005]. The criteria $\nabla \cdot \mathbf{B} = 0$ requires that B_X at the upstream boundary remain constant during the simulation. We therefore set B_Y and B_Z from the MAG data and set $B_X = 0$. Figure 1 shows the data measured by Cassini as well as a comparison with the model, which we will describe later.

[5] During approach, Cassini crossed the BS of Saturn seven times. This is most easily seen in the magnetometer

[1]Department of Atmospheric, Oceanic and Space Science, University of Michigan, Ann Arbor, Michigan, USA.
[2]Department of Physics and Astronomy, University of Iowa, Iowa City, Iowa, USA.
[3]Space and Atmospheric Physics, Imperial College, London, UK.

0094-8276/05/2005GL022835

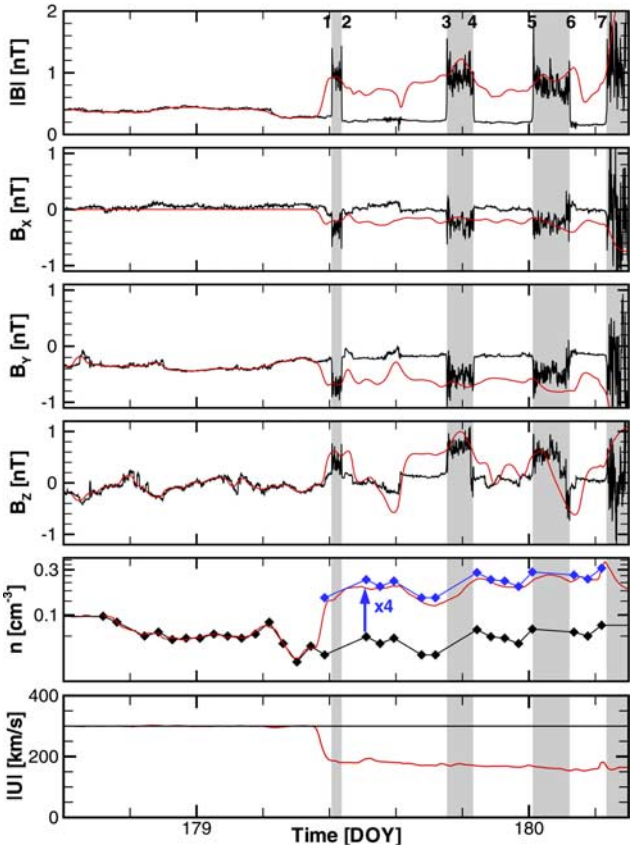

Figure 1. Comparison of MHD model output with Cassini data. Red lines represent values extracted from the MHD model at the position of Cassini. Black lines and diamonds represent values measured at Cassini. For the plasma density the RPWS instrument provided hourly values shown as diamonds, while the connecting lines indicate linear interpolations. For velocity, the black line indicates the assumed upstream constant value of 300 km/s. Periods when Cassini was in the magnetosheath are marked in gray. The times of the BS crossings are at the edges of the gray areas and are marked with numbers. In the density comparison, we also include a trace of the RPWS data multiplied by 4 (in blue). Since the RPWS data represents only plasma densities in the solar wind, multiplying by 4 represents the value behind a strong shock in the magnetosheath.

data in Figure 1 where the field magnitude shows an abrupt increase or decrease. To set the upstream solar wind boundary we must remove periods where Cassini is in the magnetosheath. For both the magnetometer and plasma density measurements we linearly interpolate across these times.

3. The MHD Model

[6] Saturn's magnetosphere is modeled using a version of the global, 3-D magnetohydrodynamic (MHD) model BATSRUS [*Powell et al.*, 1999]. The model used here is similar to the one presented in our previous Saturn model [*Hansen et al.*, 2000]. The major improvements include a substantially modified prescription of the mass loading distribution and the use of Cassini data to prescribe the upstream conditions. Other improvements include the use of the semi-relativistic form of the MHD equations [*Gombosi et al.*, 2001], an implicit time stepping algorithm based on the algorithms by *Tóth et al.* [1998], and better resolution.

[7] Because the addition of mass to the Kronian system is significant, we include this process in our model through appropriate source terms for ionization, pickup, recombination and ion-neutral drag [*Hansen et al.*, 2000]. We model the inner source due to the icy satellites as an axisymmetric torus confined near the equatorial plane using data from *Richardson and Sittler* [1990] and *Richardson et al.* [1998]. The functional form is

$$\dot{n}_I = A\dot{n}_0 e^{-(R_c-R_0)^2/H_r^2} \; e^{-z^2/H_n^2} \; e^{-z^2/H_e^2} \tag{1}$$

where $\dot{n}_0 = 8.7 \times 10^{-5}$ cm^{-3} s^{-1}, R_c is the distance from Saturn's rotational axis, $R_0 = 5.35R_S$, $H_n = 0.45R_S$ is the scale height of the water group neutral distribution and $H_e = 0.6 + 0.2(R_c - 3.0)$ is the electron scale height. The radial scaling is given by

$$H_r = \begin{cases} 1.2R_S & R_c < R_0 \\ 2.25R_S + 0.075(R_c - R_0) & R_c \geq R_0. \end{cases} \tag{2}$$

We use an average mass of 16.6 amu which assumes a nearly equal mix of OH and O. The factor A is used to scale the total mass loading rate up or down. With a nominal value of $A = 1$ the mass loading rate is $\dot{Q}_I \approx 1 \times 10^{27}$ s^{-1}.

[8] The mass loading due to Titan is also modeled as an axisymmetric torus. The torus is centered on Titan's orbit and has a much lower mass addition rate than the previous source. The functional form of our assumed neutral density is $n_N = 10.0 \exp(-r^2/H_N^2)$, where r is the distance from the center line of the torus, and $H_N = \sqrt{2}\ R_S$ [*Ip*, 1992]. This function gives a peak neutral density of 10 cm^{-3} at Titan's orbit and when combined with a neutral lifetime (3×10^7 s [*Barbosa*, 1987]) and average mass (14 amu) yields a mass loading rate of $\dot{Q}_T \approx 5 \times 10^{25}$ s^{-1}.

[9] In the simulations, the X axis is toward the Sun, with the Z axis oriented such that the magnetic dipole axis is contained in the X-Z plane. The Y axis completes the system with Y pointing "opposite" to Saturn's orbital motion. Near alignment of the rotation and dipole axes results in both being tilted 24.48° away from the Sun. The entire simulation domain covers the area $96\ R_S < X < -576\ R_S$, $-192\ R_S < Y$, $Z < 192\ R_S$. Utilizing adaptive blocks, we are able to highly resolve the inner equatorial plane while also resolving the BS, MP and tail regions appropriately. The smallest computational cells near the icy satellite mass loading region in the equatorial plane are $3/16R_S$ across while the largest cells ($6\ R_S$) are located far down tail. The inner boundary is at $3R_S$.

4. Discussion

[10] In order to match the initial BS crossing, we treat the mass loading rate and solar wind speed as free parameters. We find that a solar wind speed of 300 km/s and a mass loading rate of $\dot{Q}_I \approx 1 \times 10^{28}$ s^{-1} ($A = 11.1$) provide a good fit to Cassini's initial BS crossing (see both Figure 1 and Figure 2 (left)), however this choice is not unique. Increas-

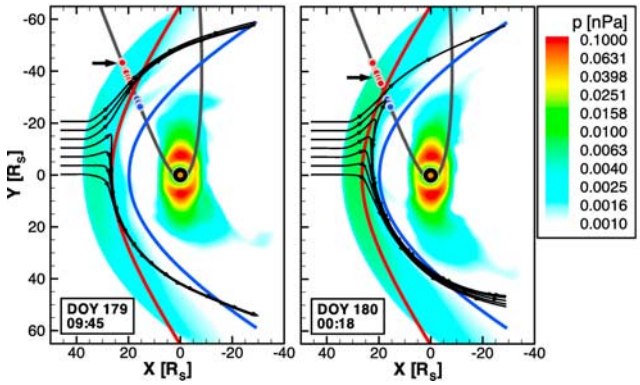

Figure 2. $Z = 0$ slices through the simulation. Color code represents the thermal plasma pressure. Near Saturn the contours are not circular due to the tilt of the equatorial plane to the $Z = 0$ plane. The gray line is a projection of Cassini's trajectory. Red dots are measured BS crossings and blue dots are measured MP crossings. The solid red and blue lines are respectively the [*Slavin et al.*, 1985] average BS and MP models. We use flow stream lines in black as a proxy for the MP. (left) The time of the first crossing for which the model was tuned. (right) The time of the fifth crossing. The inner boundary is shown as a black circle while the size of Saturn is shown as an orange circle.

ing the solar wind speed moves the BS in while increasing the mass loading rate pushes the BS out, implying that it would be possible to also match the BS crossings with both a higher solar wind speed and a higher mass loading rate. Because the solar wind speed that we use is low, the actual mass loading rate in the Saturn system may be even higher than the one used in the simulation. The rate we have used is quite high, but is comparable to recent findings of other studies [*Jurac and Richardson*, 2005; *Esposito et al.*, 2005].

[11] After the initial BS crossing, the model does not predict the additional crossings measured by Cassini; the model predicts Cassini would enter the magnetosheath at time 1 and remain there. This can be clearly seen in Figure 1 where distinct jumps in the model density and velocity occur at time 1, but no further jumps (crossings) are apparent.

[12] Many features in Figure 1 indicate that this model is accurate even though it does not predict additional shock crossings. In the figure, gray areas indicate times when measurements and model predictions both place Cassini in the magnetosheath. During these periods the model shows excellent agreement with the magnetometer data; the field magnitude is about correct and between crossings 5 and 6, for example, the B_Z component of the model correctly follows the measured field reversal. In addition, during each of these periods the magnetic field magnitude (and several components) show increases, possibly indicating that the field is being compressed and that the BS is moving inward in the model. The behavior of the model indicates that the movement of the BS is consistent with Cassini's BS crossings at times 3, 5 and 7.

[13] During periods 2–3, 4–5 and 6–7 Cassini measurements place the spacecraft in the solar wind while the MHD model predicts a location in the magnetosheath. For these times, the data and model show marked differences in the magnitudes of values, however many trends are similar. For example, the model predicts a density in the magnetosheath that is 4 times the solar wind value. This is the maximum compression ratio for strong magnetosonic shocks. In addition, there are increases in the field magnitude, as well as features in the Y and Z components in the model that "track" the data: increases, decreases or sign changes at the correct times. Because the value just inside the BS depends on both the solar wind conditions and the MHD jump conditions, one can expect the conditions just inside the BS to be closely related to the ones just outside in the solar wind. Hence the tendency of the model output to "follow" the Cassini data during these periods.

[14] The right frame of Figure 2 indicates how the shock location at future times is nearly correct. As an example, the frame shows the state of the magnetosphere at the time of the fifth shock crossing. At this time, the model predicts that Cassini should be just inside the magnetosheath. However, the model BS prediction is within $5R_S$ of the measured location.

[15] We believe that with a time history of the solar wind velocity, we would be able to match each of the BS crossings. Examining a time sequence of images like those in Figure 2 reveals the shock to be moving in and out at about the correct times but with less radial range than the measurements. A time variable solar wind velocity would yield a larger range in the dynamic pressure and in the resulting shock position. The remaining free parameter is the total mass loading rate, which could be tuned to match the crossings. Without the velocity it is possible to tune the model to match one or several of the crossings, but not all of them simultaneously.

[16] Figure 2 reveals several other features of the model. First, as a group, the BS and MP crossings are well described by the model; the BS stand-off distance from of the MP ($\sim 12R_S$) is consistent with the Cassini data. The BS and MP model of *Slavin et al.* [1985] is shown in each frame for comparison. We note that the average locations of these discontinuities computed for the Pioneer and Voyager crossings were significantly closer to Saturn than the Cassini crossings. Our MHD model is able to describe these differences. In addition, the shape of the BS and MP surfaces from the MHD simulation are different than those predicted in the *Slavin et al.* [1985] model; the MHD BS and MP are both less flared than the Slavin model, while the MHD MP is significantly asymmetric in part due to the planetary rotation.

[17] An important characteristic of our model is the tilt of the dipole and the result it has on the North-South asymmetry of the magnetosphere. Figure 3 shows the $Y = 0$ plane of the simulation at the time of Cassini's first BS crossing. The BS and MP show clear asymmetries due to the dipole tilt and the plasma density in the tilted equatorial plane. The magnetotail shows a pronounced "hinge" at the orbit of Titan ($\approx 20R_S$) due to the tilt of the rotational equator with respect to the solar wind direction.

[18] We have extracted the sub-solar BS and MP locations in order to study the stand-off distance as a function of solar wind dynamic pressure. We locate the BS at the midpoint of the MHD jump in velocity and the MP at the location of the maximum current magnitude. Both measurements are made along the x-axis and are computed every 15 minutes during the 48 hours of the

simulation centered at noon on day 179. Figure 4 shows model locations compared to BS and MP crossings measured by Pioneer 11, Voyager 1 and Voyager 2, taken from *Slavin et al.* [1985]. Because we use a constant solar wind speed, the available range of dynamic pressures (P_{sw}) is due solely to the range in solar wind plasma density. Over this range we find that the model results are quite consistent with those of *Slavin et al.* [1985], although the model consistently predicts a slightly larger standoff distance of the MP. We find that the BS and MP sub-solar locations vary as $P_{sw}^{-1/5.9}$ and $P_{sw}^{-1/5.2}$ compared respectively with $P_{sw}^{-1/5.1}$ and $P_{sw}^{-1/6.1}$ found by *Slavin et al.* [1985]. The MP value of $-1/5.2$ falls nearly in the middle of those of Jupiter ($-1/4$) and Earth ($-1/6$). This result indicates that the significant mass loading in Saturn's magnetosphere has an effect similar to Jupiter's magnetosphere. The mass makes the magnetosphere more reactive to solar wind pressure changes, however the effect is not as drastic as at Jupiter. In the figure, the scatter in MP location is likely a result of not only pressure balance, but also the past history of solar wind conditions.

5. Summary

[19] Using our MHD model of the global Saturnian magnetosphere we are able to model the period when Cassini approached and first entered the magnetosheath by treating the solar wind speed and the mass loading rate as free parameters. We find that we must use a significant mass loading rate ($\sim 1 \times 10^{28}$ s^{-1}) in order to move the bow shock far enough from Saturn to match the data. Due to our use of a low solar wind speed (300 km/s) this mass addition rate is likely a lower bound which would need to be increased if we used a larger speed.

[20] Although the model predicts only one bow shock crossing, we find a good comparison with the Cassini data throughout the modeled period (26–29 July 2004). The shock and magnetopause locations are within $5R_S$ of the measured locations and show the correct motion. Given a time series of the velocity we believe that we could correctly model the entire group of crossings.

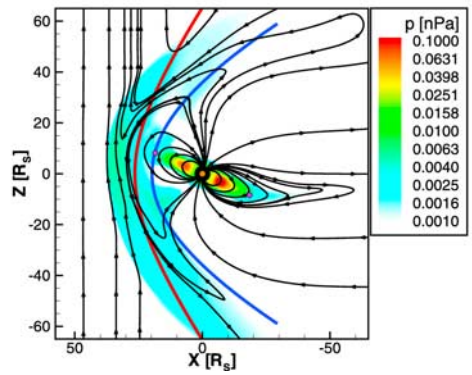

Figure 3. $Y = 0$ plane at the time of the first BS crossing. Color contour is the thermal plasma pressure with black lines representing magnetic field lines. The solid red and blue lines are the same as Figure 2. The intersection of Titan's orbit with this plane is shown as two small pink dots.

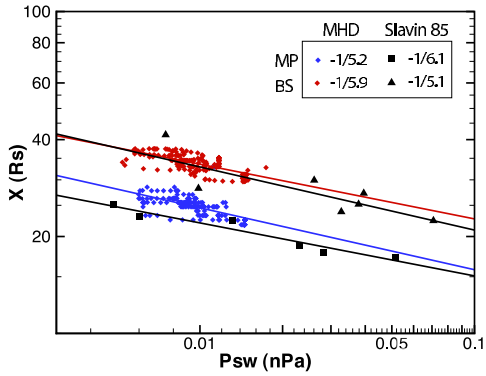

Figure 4. Comparison of BS and MP locations measured by Pioneer 11, Voyager 1 and Voyager 2 [*Slavin et al.*, 1985] with those extracted from the MHD model. Lines indicate fits to a power law of the form P_{sw}^{α}. Values for α are indicated in the figure.

[21] Finally, we find several interesting features of the magnetosphere. The bow shock, and more significantly the magnetopause, show asymmetries which are not present in the models of *Slavin et al.* [1985]. However, the dependence of the magnetopause and bow shock locations on solar wind dynamic pressure is consistent with the Pioneer 11, Voyager 1 and Voyager 2 values. The magnetopause dependence of $P_{sw}^{-1/5.2}$ lies midway between the values at Jupiter and the Earth. In addition, we find that rotation of Saturn induces dawn-dusk asymmetries in the surfaces and the magnetosphere. The tilt of the dipole results in a North-South asymmetry and produces a magnetotail which is hinged near the orbit of Titan.

[22] **Acknowledgments.** This work has been supported at the University of Michigan by the NASA Cassini Project under contract JPL-961178, NASA AISRP grant NNG04GP89G, NASA ESS CT cooperative agreement NCC5-614, and by DoD MURI grant F49620-01-1-0359. G.T. has been partially supported by the Hungarian Science Foundation (OTKA, grant No. T047042).

References

Barbosa, D. (1987), Titan's atomic nitrogen torus: Inferred properties and consequences for the Saturnian magnetosphere, *Icarus*, *72*, 53–61.

Crary, F. J., et al. (2005), Solar wind dynamic pressure and electric field as the main factors controlling Saturn's aurorae, *Nature*, *433*, 720–722.

Dougherty, M. K., et al. (2005), Cassini magnetometer observations during Saturn orbit insertion, *Science*, *307*, 1266–1270.

Esposito, L. W., et al. (2005), Ultraviolet imaging spectroscopy shows an active Saturnian system, *Science*, *307*, 1251–1255.

Gombosi, T. I., G. Tóth, D. L. De Zeeuw, K. C. Hansen, K. Kabin, and K. G. Powell (2001), Semi-relativistic magnetohydrodynamics and physics-based convergence acceleration, *J. Comput. Phys.*, *177*, 176–205.

Gurnett, D. A., et al. (2005), Radio and plasma wave observations at Saturn from Cassini's approach and first orbit, *Science*, *307*, 1255–1259.

Hansen, K. C., T. I. Gombosi, D. L. DeZeeuw, C. P. T. Groth, and K. G. Powell (2000), A 3D global MHD simulation of Saturn's magnetosphere, *Adv. Space Res.*, *26*, 1681–1690.

Ip, W. (1992), The nitrogen tori of Titan and Triton, *Adv. Space Res.*, *12*(8), 73–79.

Maurice, S., I. M. Engle, M. Blanc, and M. Skubis (1996), Geometry of Saturn's magnetopause model, *J. Geophys. Res.*, *101*, 27,053–27,060.

Powell, K. G., P. L. Roe, T. J. Linde, T. I. Gombosi, and D. L. D. Zeeuw (1999), A solution-adaptive upwind scheme for ideal magnetohydrodynamics, *J. Comput. Phys.*, *154*, 284–309.

Richardson, J. D., and S. Jurac (2004), A self-consistent model of plasma and neutrals at Saturn: The ion tori, *Geophys. Res. Lett.*, *31*, L24803, doi:10.1029/2004GL020959.

Richardson, J. D., and E. C. Sittler (1990), A plasma density model for Saturn based on Voyager observations, *J. Geophys. Res.*, *95*, 12,019–12,031.

Richardson, J. D., A. Eviatar, M. A. McGrath, and V. M. Vasyliunas (1998), OH in Saturn's magnetosphere: Observations and implications, *J. Geophys. Res.*, *103*, 20,245–20,255.

Slavin, J. A., E. J. Smith, J. R. Spreiter, and S. S. Stahara (1985), Solar wind flow about the outer planets—Gas dynamic modeling of the Jupiter and Saturn bow shocks, *J. Geophys. Res.*, *90*, 6275–6286.

Stahara, S. S., R. R. Rachiele, J. R. Spreiter, and J. A. Slavin (1989), A three dimensional gasdynamic model for solar wind flow past nonaxisymmetric magnetospheres—Application to Jupiter and Saturn, *J. Geophys. Res.*, *94*, 13,353–13,365.

Tóth, G., R. Keppens, and M. A. Botchev (1998), Implicit and semi-implicit schemes in the Versatile Advection Code: Numerical tests, *Astron. Astrophys.*, *332*, 1159–1170.

N. Achilleos and M. K. Dougherty, Space and Atmospheric Physics, Imperial College, London SW7 2BW, UK.

T. I. Gombosi, K. C. Hansen, A. J. Ridley, and G. Tóth, Department of Atmospheric, Oceanic and Space Science, University of Michigan, Ann Arbor, MI 48109, USA. (kenhan@umich.edu)

G. B. Hospodarsky, Department of Physics, University of Iowa, Iowa City, IA 52242–1479, USA.